Global Ecology and Conservation 21 (2020) e00838

Contents lists available at ScienceDirect

Global Ecology and Conservation

journal homepage: http://www.elsevier.com/locate/gecco

Original Research Article

Vertical heterogeneities of cyanobacteria and microcystin concentrations in lakes using a seasonal *In situ* monitoring station

A.A. Wilkinson [a, b], M. Hondzo [a, b, *], M. Guala [a, b]

[a] St. Anthony Falls Laboratory, University of Minnesota, Minneapolis, MN, USA
[b] Department of Civil, Environmental, and Geo- Engineering, University of Minnesota, Minneapolis, MN, USA

ARTICLE INFO

Article history:
Received 31 August 2019
Received in revised form 31 October 2019
Accepted 1 November 2019

Keywords:
Cyanobacteria
Eutrophication
Microcystin
Lakes
Physical environment
Phytoplankton

ABSTRACT

A high frequency, high resolution, seasonal research station was deployed to quantify a wide range of local meteorological conditions, water temperature, and water chemistry, including phycocyanin, in two different eutrophic stratified Minnesota lakes. The monitoring effort was coupled with discrete weekly sampling measuring nutrients, cyanobacteria composition, and microcystin concentrations. Our objective was to describe the vertical and seasonal distributions of cyanobacteria biovolume (BV) and microcystin concentrations (MC) using physical lake variables. Two types of BV distributions were observed above the thermocline upward in the water column. The first distribution depicted BV uniformly distributed over the diurnal surface layer (h_{SL}), and the second BV distribution displayed local BV maxima. A quantitative relationship was developed to determine the anticipation of observing a uniform distribution as a function of the surface layer Reynolds number (Re_{SL}), the dimensionless ratio of inertial to viscous forces. The uniform distribution was observed systematically for $Re_{SL} > 50{,}000$. MC was observed to accumulate above the thermocline and have a vertical distribution similar to BV, thus depending on Re_{SL}. This is important for directing sampling efforts, because it narrows the range of BV and MC heterogeneity above the thermocline, and suggests a vertical sampling protocol to detect potential maxima and compute representative depth-average concentrations. We explored the temporal variability of the MC to BV ratio, spatially averaged in the epilimnion (MC_{ep}/BV_{ep}). The maximum MC_{ep}/BV_{ep} occurred before the maximum BV_{ep} and specifically, during the onset of significant biomass growth in both lakes. This observation is notable because the maximum MC_{ep} occurs before the visual signs of enhanced cyanobacterial accrual are less recognizable to the public and to monitoring efforts. Our findings could have important implications for predicting MC distribution and guiding monitoring strategies for quantifying MC concentrations in small stratified lakes.

* Corresponding author. St. Anthony Falls Laboratory, University of Minnesota, Minneapolis, MN, USA.
E-mail address: mhondzo@umn.edu (M. Hondzo).

https://doi.org/10.1016/j.gecco.2019.e00838

1. Introduction

Cyanobacteria blooms are accumulations of photosynthetic microorganisms, which represent a ubiquitous nuisance in freshwater ecosystems across the world. Most studies have been focused on the large, well-known water bodies impaired from seasonal blooms, including Lake Erie in North America, Lake Taihu in China, and Lake Victoria in Africa (Wang et al., 2016). However, smaller lakes are an integral part of the fresh surface water, especially in central North America (Pannard et al., 2011). Dynamics of blooms in small to medium lakes across the globe are changing more rapidly due to changes in temperature regimes including warming surface water and strong stratification (Planas and Paquet, 2016). Additionally, smaller lakes experience a broader range of stratification conditions throughout a season, as quantified by the Lake Number or Schmidt Stability index (St) (Pannard et al., 2011; Planas and Paquet, 2016; Imberger, 2013).

Although excessive nutrients have been targeted as a management strategy to control algal blooms (Paerl et al., 2014; Gobler et al., 2016; Harke et al., 2016), they are not the sole contributor to describe the global trends in cyanobacteria bloom dynamics, particularly to explain the frequency and spatial variability of cyanobacterial concentrations (Reynolds, 1987; Song et al., 2007; JöHnk et al., 2008; Taranu et al., 2012; Molot et al., 2014; Marti et al., 2016; Planas and Paquet, 2016; Paerl, 2018). To more fully explore the spatial and temporal variabilities of cyanobacteria blooms, field investigations should include continuous diurnal observations of local meteorological conditions, water temperatures, and cyanobacteria biomass in addition to nutrients (Steinberg and Hartmann, 1988; Drakare and Liess, 2010; Cantin et al., 2011; Wang et al., 2016; Przytulska et al., 2017). In small lakes with insignificant tributary input, vertical variability of cyanobacteria biomass is much higher than that of horizontal variability across the lake surface (Marti et al., 2016; Planas and Paquet, 2016; Huisman et al., 2018). This vertical variability is very important for risk management of public drinking water intake and must be considered for both bloom sampling and remote sensing efforts (Cuypers et al., 2011).

A critical aspect of cyanobacteria blooms is their potential to produce a wide range of cyanotoxins, including microcystin, which is produced by several cyanobacteria genera like the ones observed in this study. Understanding the distribution for the toxin concentrations is important for mitigation of potential contamination of drinking water, recreational exposure, and overall ecosystem health (Carmichael, 1994). Toxin production of cyanobacteria in lakes has been recently shown to be driven by a combination of environmental factors including nutrients (Cantin et al., 2011), light (Walsby and Schanz, 2002), and temperature (Cuypers et al., 2011), which all vary with depth (Holland and Kinnear, 2013). More importantly, recent studies have shown the interplay amongst the vertical lake structure and various environmental factors in controlling cyanobacteria distribution, buoyancy, and toxicity (Song et al., 2007; Graham and Jones, 2009; Marti et al., 2016; Rowe et al., 2016). It is therefore important to consider the vertical variability of both cyanobacteria concentrations and the toxins produced.

Wilkinson et al. (2019) developed a research station that acquired high-frequency and high-resolution time series of meteorological and water quality variables. We deployed the research station in two Minnesota lakes to explore the following objectives: 1) identify the physical drivers associated with the BV vertical distribution above the thermocline, 2) describe the vertical distribution of microcystin concentrations in relation to BV and physical lake conditions, and 3) explore temporal patterns of microcystin production and BV accumulation. The results presented here are expected to be relevant for future water quality management, monitoring, and sampling strategies.

2. Methods

2.1. Research station

The long-term, high-frequency, high-resolution vertically profiling research station was deployed in Madison Lake from July to mid-August 2016, at a location with 9.2 m depth, and in South Center Lake from May to mid-August 2017, at a location with 16.7 m depth. The research station collected measurements in three forms: 1) 5-min average *in situ* local meteorological data for the wind speed, wind direction, ambient photosynthetically active radiation (PAR), precipitation, air temperature, and relative humidity; 2) 5-min average *in situ* water temperature data at 12 depths distributed over the water column; and 3) a vertical profile of water quality variables every 2 h every one meter of depth (Wilkinson et al., 2019). The meteorological data were recorded by the weather station (Campbell Scientific, Inc., UT, USA). The 12 water temperatures were recorded by the thermistors arranged on a chain (Cambell Scientific, UT, USA). The water quality variables, measured by a Hydrolab DS5 Water Quality Multiprobe (Hach Environmental, CO, USA), included the water temperature, pH, dissolved oxygen (DO), PAR, specific conductivity, and phycocyanin (a proxy for cyanobacteria concentrations). Each water quality data point was an average of 12 replicate measurements. The research station was powered by a solar charged marine battery and includes cell modem based telemetry providing real-time remote access to the station. The Campbell Scientific CR1000 data logger controlled a motorized reel that spooled the water quality multiprobe cable and allowed the controlled lowering of the multiprobe through the water column. At user-specified times (up to once per hour) and at any number of preprogrammed depths, profiles of the water quality variables were collected by lowering the multiprobe through the profiling range, stopping at each desired profile depth long enough to allow the measurements to achieve local equilibrium and statistical stationarity. The research station can be remotely operated from anywhere in the world, allowing a remote user to position the multiprobe at any desirable depth and monitor and store the measurements at the prescribed time and location. The research station had wireless data transfer, and real-time data display over the Internet.

2.2. Madison Lake

Madison Lake (coordinate 44.19056°,-93.80861°) is a residential and recreational lake located in a primarily agricultural watershed in south-central Minnesota (Fig. 1a). It is a polymictic lake with an area of 5.4 km^2, a maximum depth of 9.2 m at the measuring location, and a mean depth of 3.4 m. Because of the high nutrient inputs from its surrounding agricultural watershed, Madison Lake is classified as eutrophic (Lindon, Valley & Mackenthum, 2010). The lake was chosen as the study site because of its eutrophic classification, long water quality monitoring record, and history of frequent toxic algal blooms throughout the summer (Lindon and Heiskary, 2009).

2.3. South Center Lake

South Center Lake (coordinate 45.3716170°, −92.8275500°) is a 3.4 km^2 dimictic, eutrophic lake with a maximum depth of 36 m and a mean depth of 5.7 m (Fig. 1b). This lake has a long history of water quality monitoring and is classified by the Minnesota Pollution Control Agency (MPCA) as a eutrophic Sentinel Lake (Lindon et al., 2010). South Center Lake serves as a recreational lake with high summer boat traffic and high fishing pressure throughout the year. Note that longer records of BV, water temperatures, and meteorological data are available for South Center Lake because the research station was deployed earlier in the year.

2.4. Discrete samples

To supplement the research station measurements, discrete water samples were taken weekly with a Van Dorn sampler at the research station. Samples were collected for every meter of depth, concurrent with the profiles collected by the research station. These samples were used to evaluate local total microcystin concentration (MC), dissolved nitrate and phosphate concentrations, phycocyanin concentrations, and cyanobacteria BV and composition. To determine the vertical distribution of

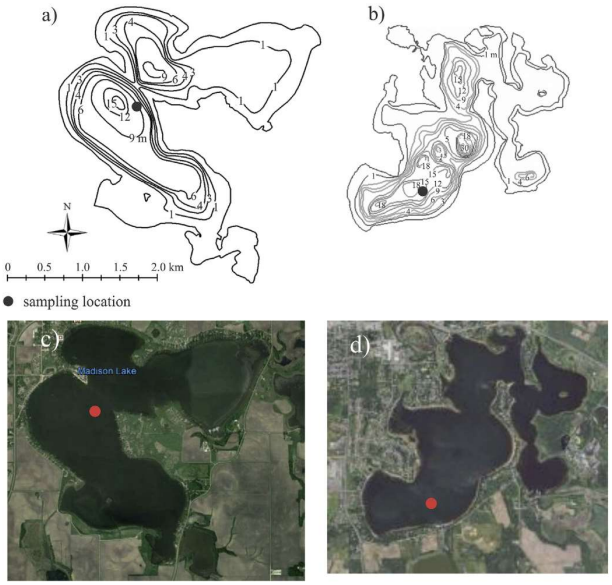

Fig. 1. a) Contour map of Madison Lake, MN (contour lines defined in meters). The circle marks the location of the floating research station during summer 2016. The depth at the measuring location was 9.2 m. b) Contour map of South Center Lake. The circle represents the location of the research station during the summer of 2017 (the depth at measuring location local was 14.0 m). c) and d) Satellite images of selected lakes.

macronutrients throughout the summer, phosphate and inorganic nitrogen concentrations were analyzed from the discrete water samples. The water samples were first filtered through GF/F filters (Whatman, Maidstone, UK) and stored at 2 °C until analyzed. The filtered water samples were measured by a laboratory bench-top fluorometer (Trilogy, Turner Designs, CA, USA P/N: 7200-0000). For phosphate concentrations, the bench-top fluorometer was augmented with a phosphate absorbance module (Trilogy, Turner Designs, CA, USA P/N: 7200-070) that accommodated a four-sided, clear 10 mm, glass square cuvette. The phosphate concentrations, [PO4], were measured according to (Parsons et al., 1984). A calibration curve was constructed using a serial dilution of potassium dihydrogen phosphate standards with concentrations ranging from 8.9 to 1138 μg/L. For the nitrate concentration, the bench-top fluorometer was similarly augmented with a nitrate absorbance module (Trilogy, Turner Designs, CA, USA (P/N: 7200-074) that accommodated the same glass square cuvette. The LaMotte nitrate test kit method, using the Nitrate-Nitrogen Model NCR (LaMotte, Chestertown, MD, USA Cat. No. 77101), was implemented to measure nitrate concentrations. A calibration curve was constructed using a serial dilution of nitrate standard (Ricca Chemical Company, Arlington, MD, USA Cat. No. 5307-16) ranging from 0.15 to 8 mg/L. The nitrate concentrations were corroborated with nitrate + nitrite concentrations collected by the Minnesota Pollution Control Agency (MPCA) during the observation periods.

2.5. Biovolume estimation and identification

The water samples for cell identification and enumeration were preserved with Lugol's iodine and stored in 2 °C upon returning from the lake (approximately 2 h after sampling). Phytoplankton species were identified and enumerated using microscopy (Nikon Eclipse E 400) with a gridded Sedgewick-Rafter counter (Wildlife Supply Co, FL, USA) at 100x magnification and using a hemacytometer at 400x magnification. There were three dominate genera of cyanobacteria including *Microcystis* spp., *Dolichospermum* spp. *and Planktothrix* spp., all microcystin producers. Cell concentrations for Microcystis spp., Nmic, Dolichospermum spp., Ndol, and Planktothrix spp., Nplk were counted using 25 (50 μL), 25 (50 μL) and 50 (1 μL) subsamples, respectively. The cell counts per subsamples ranged from: 0–3 (colony/subsample), 40–1300 (cell/subsample) and 2–15 (filaments/subsample) for Microcystis spp., Dolichospermum spp., and Planktothrix spp., respectively.

A relatively low correlation was obtained by analyzing the cell concentration (cell/mL) versus phycocyanin measured by the probe (P-Volts), which prompted the need for conversion of cell concentrations into BV (μm^3/mL) as a more representative quantification of cyanobacteria biomass in diverse populations. The BV of the corresponding sample population was estimated considering sum of the individual BV for each dominant cyanobacteria identified, and then multiplied by the cell or colony number density (cell/mL).

$$BV\left(\frac{\mu m^3}{mL}\right) = BV_{dol}\left(\frac{\mu m^3}{cell}\right) N_{dol}\left(\frac{cell}{mL}\right) + BV_{mic}\left(\frac{\mu m^3}{colony}\right) N_{mic}\left(\frac{colony}{mL}\right) + BV_{plk}\left(\frac{\mu m^3}{filament}\right) N_{plk}\left(\frac{filament}{mL}\right) \quad (1)$$

where BV is the total biovolume measured from the sample, BVdol is the average biovolume per cell of *Dolichospermum spp.*, BVmic is the average biovolume per colony of *Microcystis* spp., and BVplk is the average biovolume per filament of *Planktothrix* spp. The average biovolumes were determined using standard geometry body approximations detailed in Hillebrand et al. (1999). Specifically, *Dolichospermum* spp. and *Microcystis* spp. cells were approximated as spheres and *Planktothrix* spp. Filaments were approximated as cylinders. The average cellular volume for *Dolichospermum* spp. was estimated by analyzing micrographs using Image Processing and Analysis in Java (ImageJ, NIH) from up to 10 sub-samples from 3 representative depths for each sampling week. The three dominate genera of cyanobacteria, making up 95% of the total biovolume (μm^3/mL), were enumerated throughout the summer (Fig. 2a and Fig. 2b).

A measure of the BV variability is provided through the standard deviation of the unit biovolume (cell or colony) estimated for each water sample corresponding to a specific day and depth. The standard deviation for the BV of each genus was calculated as the standard deviation of the cell density, σ_N, multiplied by the respective average biovolume, $\overline{BV}$; i.e., $\sigma_{mic,dol,plk} = \sigma_N \times \overline{BV}$. The total standard deviation for the total BV (σ_{total}) used the standard deviation of each genus and was estimated by $\sigma_{total}=(\sigma^2_{mic}+\sigma^2_{dol}+\sigma^2_{plk})^{1/2}$ (illustrated by the vertical bars in Fig. 2c and d).

2.6. Toxin quantification

The total microcystin concentration was measured using EPA Method 546 using ADDA ELISA PN 520011, Microtiter Plate (96T) (Abraxis INC, Warminster, PA USA). The samples were collected from representative depths and times throughout the sampling season (the same used for the BV calibration in Fig. 3) and stored in the freezer until analyzed. Directly before analysis, the samples were freeze-thaw cycled three times and then filtered using GF/C filters (Whatman, Maidstone, UK). All samples were measured in duplicate. The samples and standards were vortexed before analysis. The plates were analyzed using a BioTek EL800 96 well microplate reader set to a wavelength of 450 nm (Winooski, VT, USA).

2.7. Physical lake conditions

Using the meteorological data and vertical profiles measured by the research station, we estimated several variables to quantitatively describe the physical lake conditions. The diurnal surface mixed layer (SL) is the region of relatively constant

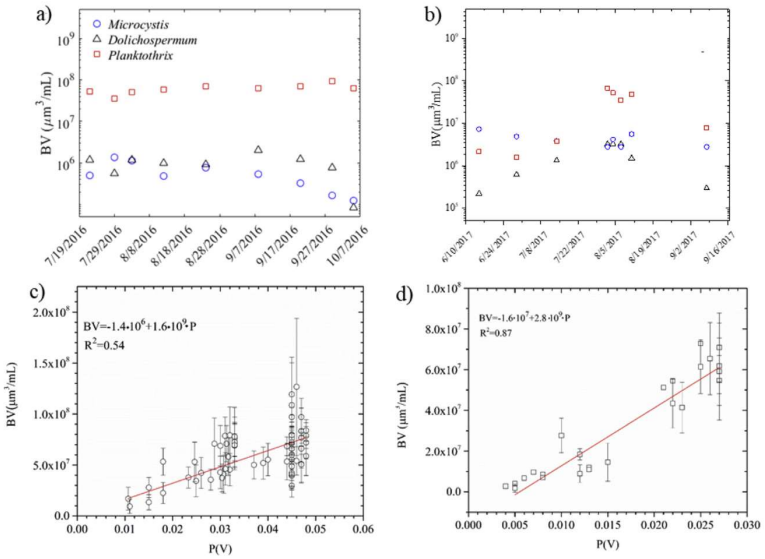

Fig. 2. a, b) Time series of dominant cyanobacteria genera BV which makes up the total BV, where the circle represents *Microcystis* sp, the triangle represents *Dolichospermum* sp, and the square represents the *Planktothrix* sp. for a) Madison Lake and b) South Center Lake. c,d) Cyanobacteria biovolume calibration with the profiling phycocyanin probe. The symbols represent an average BV from samples taken from representative depths and dates throughout the sampling effort corresponding to the phycocyanin measured, P (Voltage), by the profiling fluorometer. The vertical bars represent the standard deviation of the cell counts of each genus multiplied by the average BV of individual genera. Linear regression analyses for c) Madison Lake and d) South Center Lake yielded $BV = -1.4 \times 106 + 1.6 \times 10^5 xP$, $R^2 = 0.54$; and $BV = -1.6 \times 10^7 + 2.8 \times 10^5 xP$, $R^2 = 0.87$, respectively.

temperature at the water surface. The depth of the diurnal surface mixed layer (h_{SL}) is defined as the depth of the layer where the temperature variation remains confined within 0.3 °C from the surface temperature. The thermocline, instead, corresponds to the region of the maximum density gradient. The thermocline depth, z_T, is estimated from the density profiles by determining the first moment of the density gradient (Patterson et al., 1984; Hondzo and Stefan, 1996):

$$z_T = \frac{\int_0^{z_M} z \frac{d\rho(z)}{dz} dz}{\int_0^{z_M} \frac{d\rho(z)}{dz} dz}. \quad (2)$$

where $\rho(z)$ is the water density estimated from the temperature measured by the thermistor chain at specific depths, z, and z_M is the maximum depth.

The wind stress tilts surface water at the leeward end of the lake and generates horizontal pressure gradient which causes the tilted interface to oscillate and generate internal gravity waves which ultimately produce standing internal waves or internal seiches at the thermocline level. The seiche generates vertical oscillations of water temperature, density, and BV along the water column. The measured water temperatures must then take into account the period of internal seiche for the estimation of the local density ρ. The period of vertical mode 1 internal seiche can be estimated by the equation (Imberger, 2013):

$$t_1 = \frac{2L_T}{\sqrt{\frac{g' z_1 (z_M - z_1)}{z_M}}}. \quad (3)$$

where L_T is the basin length at the thermocline depth along the prevailing wind direction, and g' is the acceleration due to gravity compensated by the change in density between the hypolimnion, ρ_h, and the epilimnion, ρ_e, defined as: $g' = g(\rho_h - \rho_e)/\rho_h$. The seasonal seiche period was determined by estimating L_T at the average seasonal thermocline depth and g' from the averaged seasonal hypolimnion and epilimnion densities. All the meteorological and temperature data used and plotted hereinafter are averaged over the seasonal seiche period, (two and three hours for Madison Lake and South Center Lake, respectively) centered temporally on each measured profile to filter out the seiche variability and the associated internal waves.

The shear velocity at the lake surface, $u_* = (\tau_w/\rho_e)^{1/2}$, is the velocity scale derived from the shear stress at the water surface, τ_w, and is used here to quantify the effect of the wind on lake mixing and water column thermal structure. The shear stress is estimated as $\tau_w = C_D \rho_{air} U^2$, where ρ_{air} is the density of the air, the C_D is the drag coefficient (assumed to be 1×10^{-3} for $U < 5$ m/s and 1.5×10^{-3} for $U > 5$ m/s (Read et al., 2011). U is the wind speed at 10 m above the lake surface, extrapolated from the measurement height, h_w, by $U = U_h[1-(C_D^{0.5}/\kappa)\ln(10/h_w)]$, assuming a logarithmic velocity profile, $h_w = 1.5$ m is the height of the wind sensor at the floating research station providing the local wind speed U_h, and $\kappa = 0.4$ is the von Karman constant.

As a possible indicator of the thermal stability of a lake in stratified conditions, the Schmidt stability (St) was introduced and estimated using the seiche averaged temperature profiles. St describes the resistance to mechanical mixing due to the potential energy of the density stratification in the water column (Idso, 1973; Flaim et al., 2016). St is a measure of the amount of work per unit surface area needed to mix the water column to a uniform temperature, and it is defined as:

$$St = \frac{g}{A_s} \int_0^{z_M} (z - z_v)\rho(z)A(z)dz. \quad (4)$$

where A_s is the surface area of the lake, z_v is the depth at the center of the volume, and A is the basin area at depth z. As a possible indicator of wind-induced turbulent vertical mixing in the water column, a specific Reynolds number was defined using length and velocity scales of the diurnal surface mixed layer, Re_{SL}, defined as:

$$Re_{SL} = \frac{u_* h_{SL}}{\nu_{SL}}. \quad (5)$$

where u_* is the shear stress velocity, h_{SL} is the depth of the diurnal surface layer, or the extent of the nearly homogeneous water temperature from the water surface downward in the water column, and ν_{SL} is the depth-averaged kinematic viscosity of the water in the diurnal surface layer.

2.8. Statistical analyses

Statistical analyses were performed using JMP version 13.0 (SAS Institute, Cary, North Carolina, USA). One-way ANOVA was used to determine the effect of lake group variables, including the location and BV distribution, on the mean of lake response variables. One-way ANOVA analyzed the group means. If the ANOVA was significant ($\alpha = 0.05$), a Tukey Kramer HSD post hoc test was conducted. Regression analyses were performed to determine the trends between dependent and independent variables using Matlab (The MathWorks, MA, USA), and Origin (OriginLab, MA, USA).

3. Results

3.1. Meteorological and stratification conditions

The physical lake conditions measured by the research station appreciably varied throughout the study (Fig. 3). The wind speed time series depicts a cyclic pattern throughout the seasons ranging from $U = 0$ to about 6 m/s for both lakes, except for a high wind event on August 3, 2017, reaching a maximum of $U = 9$ m/s (Fig. 3a and b). In both lakes, the water temperature reached its maximum in the diurnal surface layer during July (Fig. 3c and d). Madison Lake has a higher average temperature in the water column and a more variable thermocline, consistent with the lower $\overline{St}$. South Center Lake has a much higher St than Madison Lake, with seasonally averaged values $\overline{St} = 183$ and 24 J/m^2, respectively. After August 18, Madison Lake became weakly stratified and exhibited a polymictic behavior (data not shown). Overall, the measurements suggest dimictic conditions during the sampling season in South Center Lake, quantified by high St and a persistent temperature gradient, as compared to polymictic conditions in Madison Lake, supported by highly variable thermocline depth and significantly lower St.

3.2. Water chemistry variability

Nitrate and phosphate concentrations were measured from discrete water samples from the epilimnion and hypolimnion throughout the season (Fig. 4). The phosphate concentrations were depth-averaged above the thermocline ($[PO4]_e$) and below the thermocline ($[PO4]_h$). $[PO4]_e$ was relatively constant throughout the observation period for both lakes and was high

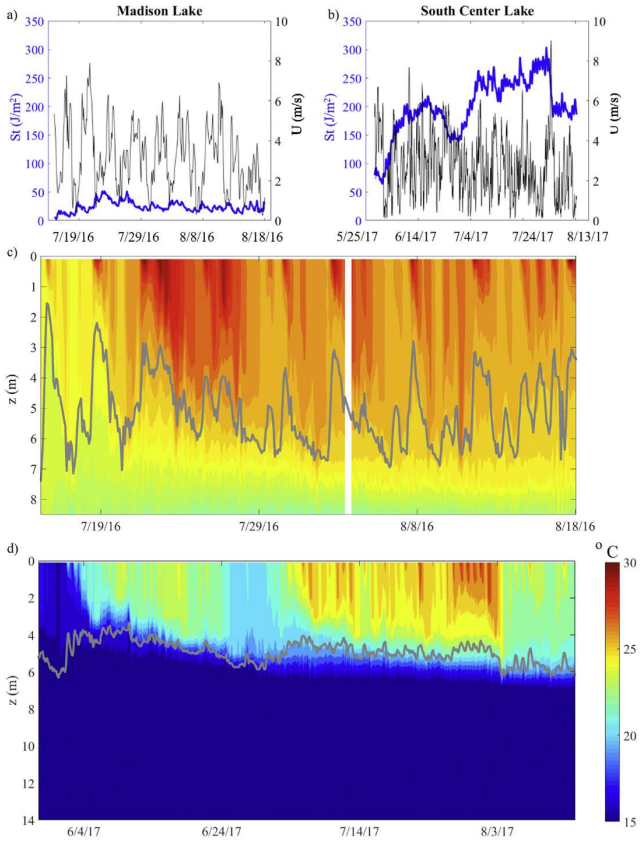

Fig. 3. Time series of wind speed U, averaged over the period of vertical mode 1 internal seiche (thin solid line) and time series of Schmidt stability index (thick line) in a) Madison Lake and b) South Center Lake. Temperature contours and the time series of thermocline depths (solid lines) for c) Madison Lake and d) South Center Lake.

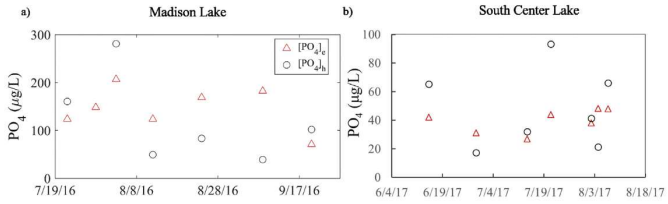

Fig. 4. Time series of average PO_4 concentrations in the epilimnion (triangles) and hypolimnion (circles) for a) Madison Lake, and b) South Center Lake.

compared to the $[PO4]_h$ in Madison Lake and comparable to $[PO4]_h$ in South Center Lake. The nitrate + nitrite concentrations measured in both the epilimnion and hypolimnion of the water column were all <0.15 mg/L (the lower detection limit of our analytical method), which is typical of Minnesota lakes (Lindon and Heiskary, 2009). Madison Lake had higher phosphate concentrations than in South Center Lake, $[PO4]_e = 150$ and 40 μg/L, respectively.

3.3. Biovolume variability

The biovolume (BV) contours show the vertical and temporal dynamics of cyanobacteria BV throughout the seasons as monitored by the profiler in Madison Lake (Fig. 5a), and South Center Lake (Fig. 5b). Both lakes experienced high BV above the thermocline, beginning in mid-July of both years. In Madison Lake, cyanobacteria accumulation extended over a larger percentage of the observed water column, and the weaker temperature gradient at the thermocline did not confine the BV as

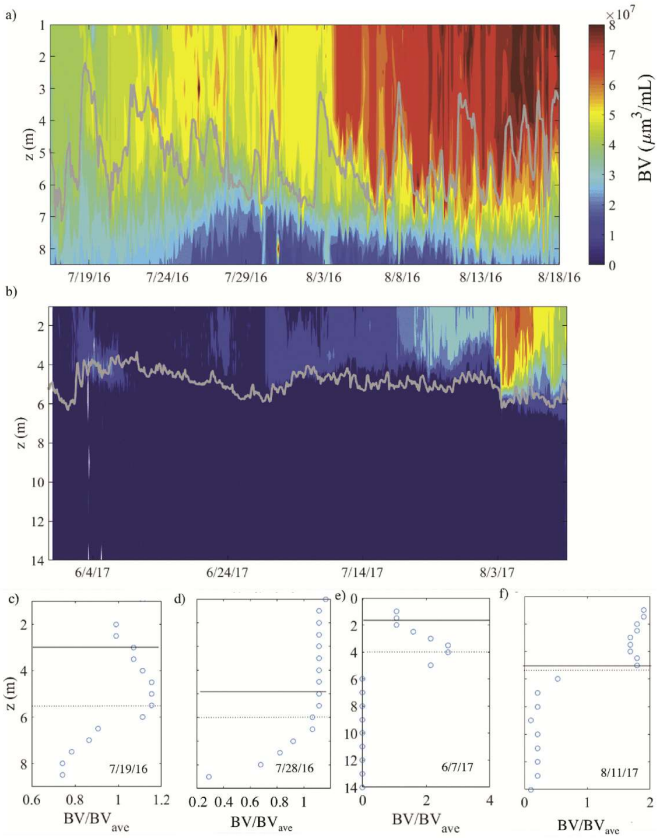

Fig. 5. Temporal contour of BV water column profiles, where the gray line is the thermocline depth for a) Madison Lake and b) South Center Lake. c-f) Selected BV profiles from c,d) Madison Lake and e,f) South Center Lake. The dotted line is the thermocline depth and the solid line is the depth of the diurnal surface layer.

Table 1
Physical lake variables consistent with BV distributions (uniform and peak) in Madison Lake and South Center Lake. μ is the mean value based on n samples, outlined below, for the respective BV distribution conditions. All variables were assessed as significant ($p < 0.05$) based on one-way ANOVA analysis and Tukey-Kramer HSD tests (JMP, SAS Institute).

	Madison Lake			South Center Lake		
	μ (uniform) n = 321	μ (peak)	p-value n = 56	μ (uniform) n = 636	μ (peak)	p-value n = 382
h_{SL} (m)	4.24	2.78	$1.1 \cdot 10^{-9}$	3.76	2.33	$4.9 \cdot 10^{-12}$
h_{SL}/z_T	0.75	0.63	$4.9 \cdot 10^{-12}$	0.65	0.48	$4.9 \cdot 10^{-12}$
u_*(m/s)	0.005	0.004	$5.2 \cdot 10^{-2}$	0.004	0.003	$4.1 \cdot 10^{-3}$
Re_{SL}	2.4×10^4	1.2×10	$1.2 \cdot 10^{-9}$	1.64×10^4	7.26×10^3	$4.9 \cdot 10^{-12}$

well as that observed in South Center Lake, resulting in higher BV in the hypolimnion. In South Center Lake on August 3, 2017, during a high wind event, the BV abruptly increased above the thermocline, which was likely due to horizontal transport of cyanobacteria by the wind. This abrupt increase is also observed by comparing the water samples taken on August 2 and on August 4, when *Planktothrix* sp. composition increases (Fig. 2b). After the wind event high BV persisted for one week and then decreased.

Overall, both Madison Lake and South Center lake are eutrophic lakes but had nitrite + nitrate concentrations <0.15 mg/L during the study periods. The main differences observed between these two lakes are 1) the higher phosphate concentrations in Madison lake, 2) the weaker thermal stability, or lower St, in Madison lake leading to a turnover in mid-August, and 3) the higher BV concentrations in Madison Lake, though with a lower contribution by *Microcystis* sp. Despite those differences, both lakes show a significant increase in cyanobacteria biovolume in early August.

3.4. Quantification of biovolume vertical heterogeneity

Despite the difference cyanobacteria composition and lake thermal stratification, high biovolume remained confined above the thermocline, in both lakes. We distinguish between two types of BV profiles above z_T: 1) uniform distribution and 2) BV distribution with a local maximum. The classification is based on the relative cyanobacteria biovolume (BV_r) and is defined as:

$$BV_r = \frac{BV_{max}}{BV_{SL}} \tag{6}$$

where BV_{max} is the maximum biovolume of cyanobacteria above the thermocline (not including thermocline) up to the water surface, and BV_{SL} is the concentration of cyanobacteria averaged over the diurnal surface layer. If $BV_r \leq 1.1$, the profile was labeled as a uniform, and if $BV_r \geq 1.2$ the profile was classified as the peak profile. There is no restriction on BV_{max} regarding the occurrence over the vertical profile above the thermocline. The visual inspection of profiles appears to be a good classification method. Examples of uniform profiles are depicted in Fig. 5d and f, and the examples of profiles with peak are displayed in Fig. 5c and e. Uniform distributions made up 62% and 85% of the BV profiles in South Center Lake and Madison Lake, respectively.

We examined physical lake variables relevant to the surface layer above the thermocline where the highest BV values were predominantly observed (Table 1). The statistical analysis of each response variable (h_{SL}, h_{SL}/z_T, u_*, Re_{SL}) was evaluated considering four groups including two different lakes, uniform, and peak distributions of BV above the thermocline. The group means were analyzed by one-way ANOVA and followed by the Tukey Kramer HSD test. Each response variable included six comparison groups. Most of the means were statistically different ($p < 0.05$). The mean of Reynolds number, Re_{SL}, was statistically different for all group combinations except for the means for the peak distributions in Madison Lake and South Center Lake. The mean values for h_{SL}, u_*, and Re_{SL} were larger for uniform distributions as compared to peak distributions in both lakes, suggesting stronger mixing due to high wind, deepening the surface mixed layer (Fig. 6 and Table 1). Since the product of h_{SL} and u_* integrates the effects of the characteristic length scale (h_{SL}) and characteristic velocity scale (u_*) of the diurnal surface layer, we combine these variables and define a Reynolds number Re_{SL} (Equation (5)).

To quantify the mechanisms governing cyanobacteria distribution in the water column, we explored results from both lakes and systematically compared the occurrence of uniform and peak distributions as a function of Re_{SL} (Fig. 7). Uniform BV distributions were observed more frequently under strong wind, at larger Re_{SL} (Fig. 7a). In particular, estimating the value of Re_{SL} from meteorological and thermal sensors, we can predict how frequently the BV distribution will be uniform or exhibiting a local peak in the epilimnion. For example, when $Re_{SL} > 5 \times 10^4$ the BV was always observed to be uniformly distributed (Fig. 7b). Conversely, for (lower) $Re_{SL} = 7 \times 10^3$ there is a 50% chance of finding a uniform or a peak distribution. The discovery of peak distribution at the lake surface is appealing since the surface blooms pose the greatest risk for the exposure to toxins. The relationship provided in Fig. 7b describes how often we expect significant BV vertical heterogeneities in the epilimnion as a function of easily measurable local meteorological and temperature variables describing the turbulent regime in the diurnal surface layer. It is important to note that St and Lake Number, which can be used to describe vertical stability of the entire water column (Imberger, 2013), were not found to be compelling in this analysis.

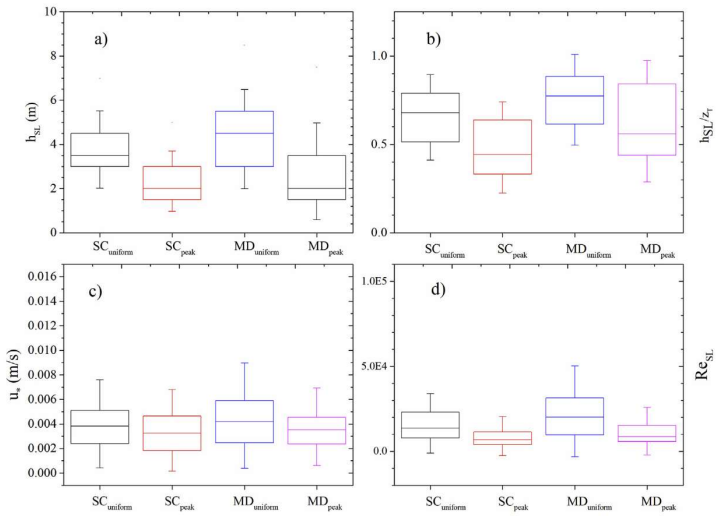

Fig. 6. Comparison between physical lake variables a) h_{SL}, b) h_{SL}/z_T, c) u_*, d) Re_{SL}, versus uniform and peak BV distributions for South Center Lake (SC) and Madison Lake (MD). The horizontal line in the box represents the median of the respective data sets. The top of the box represents the 75th percentile, the bottom of the box represents the 25th percentile and the whiskers represent 1.5 x standard deviation range of the data set.

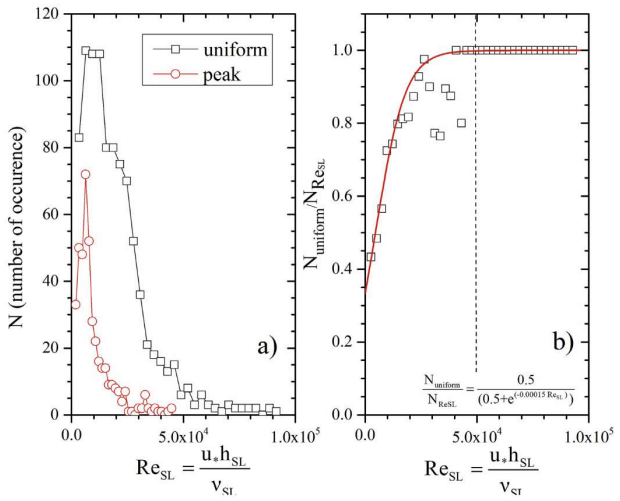

Fig. 7. a) Frequency of peak (circle symbol) and uniform (square symbol) BV distributions as a function of Re_{SL}. b) The ratio of uniform distributions to a total number of profiles as a function of Re_{SL}. These data represent all profiles for both lakes.

3.5. Microcystin and cyanobacteria biovolume vertical stratification

BV and MC profiles corresponding to selected sampling dates and depths from the epilimnion to the hypolimnion are depicted in Fig. 8. For the selected dates, a nearly uniform BV distribution was observed in the diurnal surface layer, decaying with a steep gradient in the proximity of the thermocline z_T. For both lakes, similar patterns in the distribution of BV and MC were observed. However, Madison Lake exhibits low MC concentrations that are close to the detection limit and are therefore more noisy profiles. The vertical microcystin distributions extracted from the water samples depict similar pattern to the BV profiles for all the monitored days: MC is fairly homogeneous in the diurnal surface mixed layer and negligible below the thermocline, which is then used to normalize the depth (Fig. 9).

Based on the above observations, we explore the overall relationship between MC and BV measured from the discrete samples (Fig. 10). Linear regression between MC and BV emerged from both South Center Lake and Madison Lake data. The data encompassed a wide range of depths, atmospheric conditions, BV and MC concentrations, and composition of cyanobacteria. The linear trend, quantified over the entire measuring season, was statistically more significant in South Center Lake ($R^2 = 0.78$) in comparison to Madison Lake ($R^2 = 0.36$).

The temporal variabilities of the average BV in the epilimnion (BV_{ep}) are depicted for both lakes in Fig. 11a and b. Both lakes show similar patterns of BV accrual from May to August during the two different measuring seasons. Temporal variability in the ratio of average MC in the epilimnion, to average BV in the epilimnion (MC_{ep}/BV_{ep}), were observed consistently in the two seasons (Fig. 11c). In both lakes, the maximum MC_{ep}/BV_{ep} preceded the maximum BV in the epilimnion (Fig. 11a and b). This trend was observed over a similar period (from July 14th to August 11th) in the two lakes, despite the different years and different environmental conditions.

In South Center Lake the maximum ratio occurs at the beginning of the BV_{ep} growth (Fig. 11b). Note that in Madison Lake the first MC sample was taken on July 14, which did not allow to encompass the same seasonal MC_{ep}/BV_{ep} evolution as compared to South Center Lake. Based on the two lakes data, it is likely that we missed the microcystin peak along with the onset of BV_{ep} growth.

4. Discussion

The objective of our study was to explore possible relationships among distributions of cyanobacteria biovolume (BV), microcystin concentrations (MC), lake physical variables, and meteorological conditions in two eutrophic stratified lakes. The

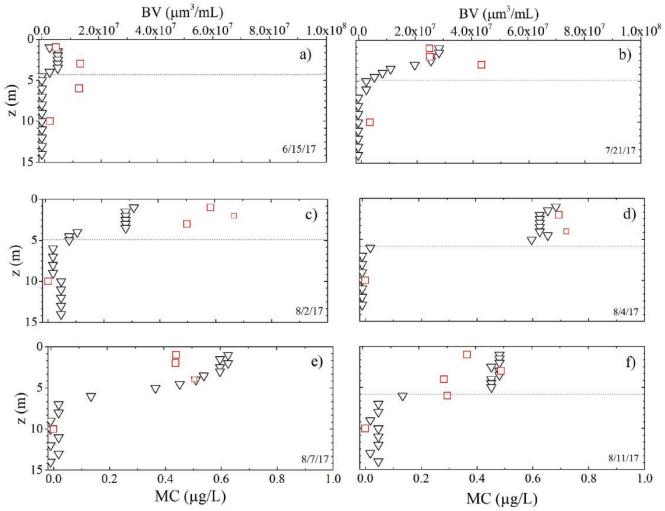

Fig. 8. Depth profiles of BV (inverted triangle symbol) and the corresponding profiles of MC (square symbol) in South Center Lake. Each MC data point is an average of duplicate samples. The dashed line represents the thermocline depth.

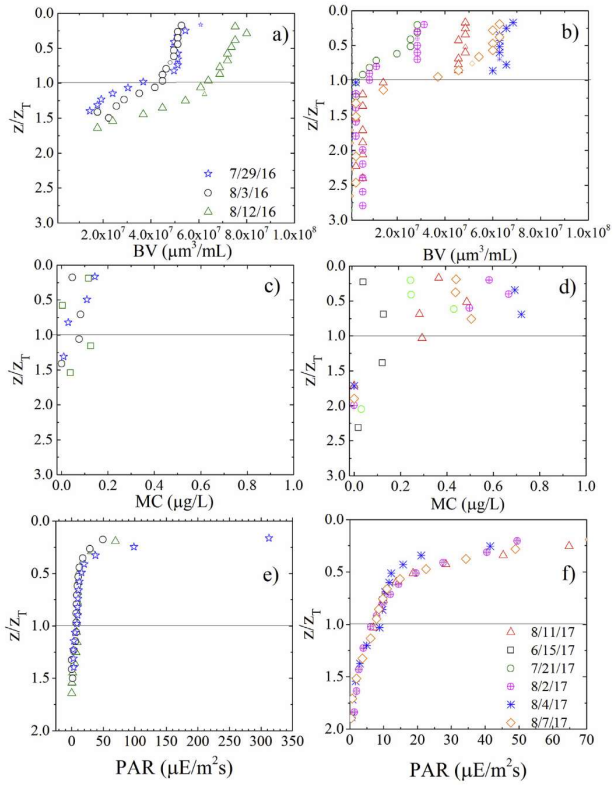

Fig. 9. Vertical BV and MC profiles normalized by the thermocline depth z_T from samples throughout the season in Madison Lake (a, c, e) and South Center Lake (b, d, f). Each MC data point is an average of duplicate samples. The horizontal line represents the thermocline depth.

predominant concentration of cyanobacteria biomass was observed above the thermocline. We further distinguish between two distributions 1) uniformly distributed BV in the diurnal surface mixed layer and 2) local maxima of the BV profile within the epilimnion. These different distributions have been shown to depend on physical lake variables including lake thermal structure and the wind speed, which control mixing in the diurnal surface layer. In particular, under large shear velocity, u_*, the water in the epilimnion is mixed to a homogeneous temperature which extends deeper in the water column, increasing the diurnal surface mixed layer depth h_{SL}. Given that $u_* h_{SL}$ consistently increased with the surface mixing and with uniform BV distribution, we defined a Reynolds number $Re_{SL}=u_* h_{SL}/\nu_{SL}$ to describe wind-induced mixing in the diurnal surface layer. Uniform BV distributions are observed under highly dynamic lake conditions, characterized by large values of u_*, h_{SL}, and Re_{SL}, demonstrating that uniform BV distributions are governed by mechanical mixing, while the cyanobacteria behaved more like passive tracers. Conversely, peak BV distributions correspond to more calm conditions, lower values of u_*, h_{SL}, and Re_{SL}, implying that cyanobacteria may be able to actively choose their location in the water column, forming high BV layers both near the surface or just above the thermocline, and obeying their physiological drivers (Steinberg and Hartmann, 1988).

The importance of wind stress, h_{SL}, and thermal structure in polymictic Lake Erie for the *Microcystis* buoyancy and their vertical distribution was reported by Rowe et al. (2016). Although our study was conducted in two small stratified lakes

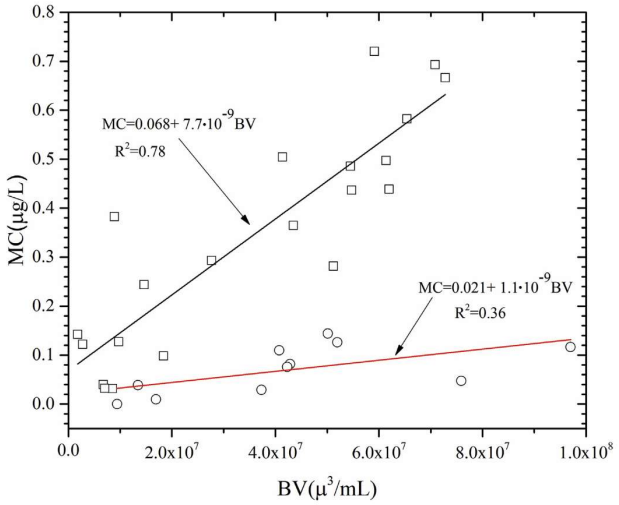

Fig. 10. Concentration of MC versus BV in South Center Lake (square symbol) and Madison Lake (circle symbol). The data points represent the average of a replicate of MC.

during the summer months, the results re-emphasized the importance of u_*, h_{SL}, and Re_{SL} to the vertical distribution of cyanobacteria in the water column. Wang et al. (2016) determined that the greatest influence of wind to cyanobacteria blooms is by direct transport throughout the water column and less by indirect nutrient transport by shear from the sediments or direct shear on individual cells. This direct transport impact was based on the critical wind speed of >2−3 m/s to disperse *Microcystis* surface blooms in the water column (Webster and Hutchinson, 1994). Additionally, the vertical distribution of *Microcystis* is particularly sensitive to the wind as compared to other phytoplankton, e.g. the vertical heterogeneity of *Microcystis* was observed to be correlated with strong winds in Lake Taihu (Cao et al., 2006). To incorporate both thermal

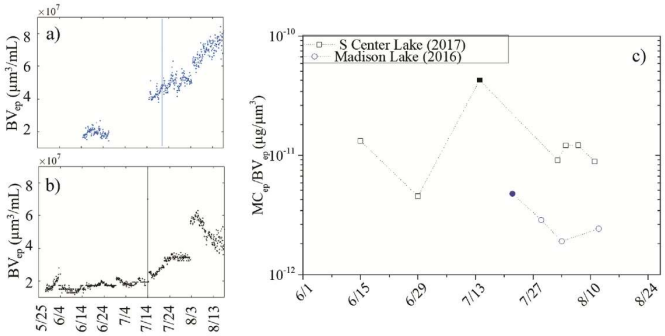

Fig. 11. Average biovolume in the epilimnion, BV_{ep}, for a) Madison Lake and b) South Center Lake. c) The time series of MC_{ep}/BV_{ep} for Madison lake (square) and South Center lake (circle). The maxima MC_{ep}/BV_{ep} are the filled symbols in c) and correspond to the dates marked by the vertical lines in panels a) and b).

structure and wind, we developed a relationship in polymictic and dimictic lakes that may predict the anticipation of the BV distribution type as a function of Re_{SL}. For a given Re_{SL} we know the anticipation of a single depth sample being representative of the BV in the surface layer, i.e. a uniform distribution. Conversely, if there is a clear peak in the BV distribution, a single depth sample is not likely to capture the maximum BV in the water column: peaks were observed to exhibit local BV up to 2 times the depth-averaged values BV_{ave} (Fig. 5). Understanding the BV distribution above the thermocline is important in determining, how representative a single depth sample is, based on a ratio of easily measurable local meteorological and temperature parameters.

The distribution of MC is consistent with the distribution of BV during the stratified period in each lake. BV and MC were concentrated above the thermocline and exhibited linear trends over different depths, dates, and local physical conditions. Graham and Jones (Graham and Jones, 2009) also showed uniform distributions of MC and cyanobacteria biomass concentrated above the thermocline and declining in deeper layers. Likewise, there was a high correlation between local cyanobacteria BV and microcystin concentrations, (Pawlik-Skowrońska et al., 2004; Graham and Jones, 2009). This said the total MC concentrations were lower in Madison Lake, likely due to the difference in cyanobacterial composition. There was much lower *Microcystis* sp biovolume contribution in Madison Lake, while the total BV was dominated by *Planktothrix* sp. Although it is a microcystin producing genera, *Planktothrix* biovolume has been shown not to be correlated with MC (Pawlik-Skowrońska et al., 2004). Additionally, high Anatoxin concentrations in Madison Lake were measured by MPCA during our sampling period (though in different locations in the lake). Anatoxin is not produced by *Microcystis* but by *Dolichospermum* spp. along with other cyanobacteria not dominant here. Chia et al. (2016) showed that exposure to Anatoxin reduced the MC production of *Microcystis*. A nationwide study of 1161 lakes found that it was very rare to observe co-production of different cyanotoxins in cyanobacteria blooms (Loftin et al., 2016).

The linear trend between MC and BV concentrations and distributions allows for the use of models describing BV vertical heterogeneities, e.g. as discussed in Wilkinson et al. (2019), to predict MC vertical distributions, even though *in situ* calibration is still necessary to determine the slope. There are several reasons behind the observed differences, involving cyanobacteria composition, physiological interactions between species, lake geometry and stratifications effects, in addition to potential delays between BV and MC time histories. The temporal variations of cyanobacteria biovolume in the epilimnion (BV_{ep}) were appreciable during the monitoring period. We observed that the peak of MC_{ep}/BV_{ep} occurred before the maximum BV_{ep}, with MC_{ep}/BV_{ep} decreasing as the high BV_{ep} persisted. In South Center Lake, this peak coincided with the onset of significant BV_{ep} increase. The MC concentrations were similar before the maximum BV concentrations as after the onset of high BV concentrations. Overall, it was notable that the trends of MC_{ep}/BV_{ep} between Madison Lake and South Center Lake were similar in shape and occurred on the comparable dates one year apart and under two different stratification conditions. This trend of MC_{ep}/BV_{ep} can also provide insight about the relationships between physiological conditions and metabolic activities of cyanobacteria in lakes (like nitrogen regulation, allopathy and the defense against grazing (Orr and Jones, 1998; Holland and Kinnear, 2013). Long et al. (Long et al., 2001) showed a linear trend between *Microcystis* growth rate and microcystin production in N-limited cultures. Similarly, Orr and Jones (1998) showed that toxin production was associated with periods of cell concentration increases not in the stationary or death phase in N-limited cultures. These results are relevant to both lakes, in fact exhibiting low inorganic nitrogen. These observations are notable because the maximum MC_{ep}/BV_{ep} occurred in periods just before the period of precipitous BV growth in the epilimnion, which is when the physical signs of harmful algal blooms are less recognizable to the public and biomass monitoring systems. Exploring the temporal lag between BV growth and MC peak concentration remains an important research question for the prediction and mitigation of cyanobacterial blooms.

Our work addresses cyanobacteria vertical heterogeneity models by describing BV distributions specifically above the thermocline. The modeling framework facilitates to use easily measurable, local, thermal and meteorological conditions in the water column, as a predictor for BV and MC vertical distributions, and thus as a guideline for water sampling strategies. The proposed analysis promotes a better understanding of cyanobacterial dynamics and probability of HAB occurrence (risk) in an individual lake.

5. Conclusion

A high frequency, high resolution, a long-term monitoring station was deployed during summer months, in a eutrophic, polymictic Minnesota lake in 2016 and a eutrophic, dimictic Minnesota lake in 2017. Although the two lakes exhibited different stratification conditions, nutrient concentrations, and cyanobacteria compositions, similar trends in both lakes unveiled functional relationships between a) wind-induced hydrodynamic mixing, b) thermal stratification, c) cyanobacteria biovolume (BV) vertical distribution, and d) microcystin (MC) vertical distribution. The biovolume distribution was observed to be influenced by wind-induced mixing in the epilimnion, frequently able to homogenize the diurnal surface layer (SL) in terms of water temperature, biovolume, and microcystin. A quantitative relationship was developed here to determine the anticipation of observing a uniform distribution in the SL as a function of the ratio of easily measurable local environmental variables. Uniform BV distributions were associated with SL Reynolds number $Re_{SL} > 50{,}000$ values consistent with greater mixing in the diurnal surface mixed layer. At lower values, cyanobacteria are inferred to be able to move along the water column, driven by physiology, enabled by buoyancy regulation, and not passively advected by the flow. This understanding is important for directing sampling efforts because it narrows the range of BV heterogeneity above the thermocline and suggests a more (or less) detailed vertical sampling protocol to capture (or neglect) potential peaks and compute representative averages at a minimal cost. This is of utmost importance because BV versus MC concentrations in each layer of the water column

could be linearly related, neglecting potential time lags as a first approximation. The key parameter for toxin evolution is identified as the MC production per unit of biovolume, quantified by the term MC_{ep}/BV_{ep} averaged in the epilimnion. Its temporal variations were monitored in both lakes and showed a maximum value occurring before the maximum BV, and likely corresponding to the onset of BV growth (especially evident from South Center Lake data). This observation is notable because the maximum MC_{ep}/BV_{ep} occurs before substantial BV accumulation when the physical signs of harmful algal blooms are less recognizable to the public and to surface monitoring efforts. Particular care must be then devoted to water sampling, when optimal lake conditions for BV growth, as those identified by Wilkinson et al. (2019), are achieved. The results presented here shed additional light on the complexity of BV and microcystin distributions and could have important implications for future management, restoration, and monitoring strategies in small stratified lakes.

Declaration of competing interest

No conflict of interest.

Acknowledgments

We acknowledge the assistance of Dr. Christopher Ellis, Ben Erickson, and the technical staff at St. Anthony Falls Laboratory for the development, maintenance and design of the research station. The authors would like to thank Jiaqi You and Jacqueline Taylor for help with data collection. For help with public outreach and coordination, we would like to acknowledge Dr. Shahram Missaghi and the Madison Lake Association. The Minnesota Pollution Control Agency provided help with research station deployment and maintenance as well as providing inorganic nitrogen data and we are very grateful. We would like to thank Dr. Christine Salomon for use of ELISA analysis equipment. Funding was provided, in part by, the Legislative-Citizen Commission on Minnesota Resources (LCCMR), Environment and Natural Resources Trust Fund 2015–2016, Assessing the Increasing Harmful Algal Blooms in Minnesota Lakes, ID: 038-B. The authors confirm there are no potential sources of conflict of interest, financial or otherwise.

References

Cantin, A., Beisner, B.E., Gunn, J.M., Prairie, Y.T., Winter, J.G., 2011. Effects of thermocline deepening on lake plankton communities. Can. J. Fish. Aquat. Sci. 68, 260–276.
Cao, H.-S., Kong, F.-X., Luo, L.-C., Shi, X.-L., Yang, Z., Zhang, X.-F., et al., 2006. Effects of wind and wind-induced waves on vertical phytoplankton distribution and surface blooms of *Microcystis aeruginosa* in lake Taihu. J. Freshw. Ecol. 21, 231–238.
Carmichael, W.W., 1994. The toxins of cyanobacteria. Sci. Am. 270, 78–86.
Chia, M.A., Cordeiro-Araújo, M.K., Lorenzi, A.S., Bittencourt-Oliveira, M. do C., 2016. Does anatoxin-a influence the physiology of Microcystis aeruginosa and Acutodesmus acuminatus under different light and nitrogen conditions? Environ. Sci. Pollut. Control Ser. 23, 23092–23102.
Cuypers, Y., Vinçon-Leite, B., Groleau, A., Tassin, B., Humbert, J.F., 2011. Impact of internal waves on the spatial distribution of Planktothrix rubescens (cyanobacteria) in an alpine lake. ISME J. 5, 580–589.
Drakare, S., Liess, A., 2010. Local factors control the community composition of cyanobacteria in lakes while heterotrophic bacteria follow a neutral model: neutral community models and local factors. Freshw. Biol. 55, 2447–2457.
Flaim, G., Eccel, E., Zeileis, A., Toller, G., Cerasino, L., Obertegger, U., 2016. Effects of re-oligotrophication and climate change on lake thermal structure. Freshw. Biol. 61, 1802–1814.
Gobler, J.C., Burkholder, M.J., Davis, W.T., Harke, J.M., Johengen, T., Stow, A.C., Van De Waal, B.D., 2016. The dual role of nitrogen supply in controlling the growth and toxicity of cyanobacterial blooms. Harmful Algae 54, 87–97.
Graham, J.L., Jones, J.R., 2009. Microcystin in Missouri reservoirs. Lake Reservoir Manag. 25, 253–263.
Harke, J.M., Steffen, M.M., Gobler, J.C., Otten, G.T., Wilhelm, W.S., Wood, A.S., Paerl, W.H., 2016. A review of the global ecology, genomics, and biogeography of the toxic cyanobacterium, Microcystis spp. Harmful Algae 54, 4–20.
Hillebrand, H., Dürselen, C.-D., Kirschtel, D., Pollingher, U., Zohary, T., 1999. Biovolume calculation for pelagic and benthic microalgae. J. Phycol. 35, 403–424.
Holland, A., Kinnear, S., 2013. Interpreting the possible ecological role(s) of cyanotoxins: compounds for competitive advantage and/or physiological aide? Mar. Drugs 11, 2239–2258.
Hondzo, M., Stefan, H.G., 1996. Long-term lake water quality predictors. Water Res. 30, 2835–2852.
Huisman, J., Codd, A.G., Paerl, W.H., Ibelings, W.B., Verspagen, M.H.J., Visser, M.P., 2018. Cyanobacterial blooms. Nat. Rev. Microbiol. 16, 471–483.
Idso, S.B., 1973. On the concept of lake stability1. Limnol. Oceanogr. 18, 681–683.
Imberger, J., 2013. Environmental Fluid Dynamics: Flow Processes, Scaling, Equations of Motion, and Solutions to Environmental Flows. *Academic Press*, Elsevier Inc., p. 430p
JöHnk, K.D., Huisman, J., Sharples, J., Sommeijer, B., Visser, P.M., Stroom, J.M., 2008. Summer heatwaves promote blooms of harmful cyanobacteria. Glob. Chang. Biol. 14, 495–512.
Lindon, M., Heiskary, S., 2009. Blue-green algal toxin (microcystin) levels in Minnesota lakes. Lake Reservoir Manag. 25, 240–252.
Lindon, M., Valley, R., Mackenthum, S., 2010. Sentinel Lake Assessment Report Madison Lake (07-0044) Blue Earth County, Minnesota.
Loftin, K.A., Graham, J.L., Hilborn, E.D., Lehmann, S.C., Meyer, M.T., Dietze, J.E., et al., 2016. Cyanotoxins in inland lakes of the United States: occurrence and potential recreational health risks in the EPA National Lakes Assessment 2007. Harmful Algae 56, 77–90.
Long, B.M., Jones, G.J., Orr, P.T., 2001. Cellular microcystin content in N-limited Microcystis aeruginosa can Be predicted from growth rate. Appl. Environ. Microbiol. 67, 278–283.
Marti, C.L., Imberger, J., Garibaldi, L., Leoni, B., 2016. Using time scales to characterize phytoplankton assemblages in a deep subalpine lake during the thermal stratification period: lake Iseo, Italy: phytoplankton assemblages IN lake iseo. Water Resour. Res. 52, 1762–1780.
Molot, L.A., Watson, S.B., Creed, I.F., Trick, C.G., McCabe, S.K., Verschoor, M.J., et al., 2014. A novel model for cyanobacteria bloom formation: the critical role of anoxia and ferrous iron. Freshw. Biol. 59, 1323–1340.
Orr, P.T., Jones, G.J., 1998. Relationship between microcystin production and cell division rates in nitrogen-limited Microcystis aeruginosa cultures. Limnol. Oceanogr. 43, 1604–1614.
Paerl, W.H., Gardner, S.W., McCarthy, J.M., Peierls, L.,B., Wilhelm, W.S., 2014. Algal blooms: noteworthy nitrogen. Sci. Lett. 346 (October 10), 175-175.
Paerl, W.H., 2018. Mitigating toxic planktonic cyanobacterial blooms in aquatic ecosystems facing increasing anthropogenic and climate pressures. Toxins 10, 76–92.

Pannard, A., Beisner, B.E., Bird, D.F., Braun, J., Planas, D., Bormans, M., 2011. Recurrent internal waves in a small lake: potential ecological consequences for metalimnetic phytoplankton populations: vertical internal modes in a small lake. Limnol. Oceanogr. Fluids Environ. 1, 91–109.
Parsons, T.R., Maita, Y., Lalli, C.M., 1984. A Manual of Chemical and Biological Methods for Seawater Analysis, first ed. Pergamon Press, Oxford [Oxfordshire] ; New York.
Patterson, J.C., Hamblin, P.F., Imberger, J., 1984. Classification and dynamic simulation of the vertical density structure of lakes1: dynamic simulation of lakes. Limnol. Oceanogr. 29, 845–861.
Pawlik-Skowrońska, B., Skowroński, T., Pirszel, J., Adamczyk, A., 2004. Relationship between cyanobacterial bloom composition and anatoxin-A and microcystin occurrence in the eutrophic dam reservoir (SE Poland). Pol. J. Ecol. 52, 479–490.
Planas, D., Paquet, S., 2016. Importance of climate change-physical forcing on the increase of cyanobacterial blooms in a small, stratified lake. J. Limnol. 75, 201–214.
Przytulska, A., Bartosiewicz, M., Vincent, W.F., 2017. Increased risk of cyanobacterial blooms in northern high-latitude lakes through climate warming and phosphorus enrichment. Freshw. Biol. 62, 1986–1996.
Read, J.S., Hamilton, D.P., Jones, I.D., Muraoka, K., Winslow, L.A., Kroiss, R., et al., 2011. Derivation of lake mixing and stratification indices from high-resolution lake buoy data. Environ. Model. Softw 26, 1325–1336.
Reynolds, C.S., 1987. Cyanobacterial Water-Blooms, Advances in Botanical Research 13. Academic Press, London, pp. 67–143.
Rowe, M.D., Anderson, E.J., Wynne, T.T., Stumpf, R.P., Fanslow, D.L., Kijanka, K., Vanderploeg, H.A., Strickler, J.R., Davis, T.W., 2016. Vertical distribution of buoyant Microcystis blooms in a Lagrangian particle tracking model for short-term forecasts in Lake Erie. J. Geophys. Res. Oceans 121, 5296–5314.
Song, L., Chen, W., Peng, L., Wan, N., Gan, N., Zhang, X., 2007. Distribution and bioaccumulation of microcystins in water columns: a systematic investigation into the environmental fate and the risks associated with microcystins in Meiliang Bay, Lake Taihu. Water Res. 41, 2853–2864.
Steinberg, C.E.W., Hartmann, H.M., 1988. Planktonic bloom-forming Cyanobacteria and the eutrophication of lakes and rivers. Freshw. Biol. 20, 279–287.
Taranu, Z.E., Zurawell, R.W., Pick, F., Gregory-Eaves, I., 2012. Predicting cyanobacterial dynamics in the face of global change: the importance of scale and environmental context. Glob. Chang. Biol. 18, 3477–3490.
Walsby, A.E., Schanz, F., 2002. Light-dependent growth rate determines changes in the population of Planktothrix rubescens over the annual cycle in Lake Zürich, Switzerland. New Phytol. 154, 671–687.
Wang, H., Zhang, Z., Liang, D., du, H., Pang, Y., Hu, K., et al., 2016. Separation of wind's influence on harmful cyanobacterial blooms. Water Res. 98, 280–292.
Webster, I.T., Hutchinson, P.A., 1994. Effect of wind on the distribution of phytoplankton cells in lakes revisited. Limnol. Oceanogr. 39, 365–373.
Wilkinson, A.A., Hondzo, M., Guala, M., 2019. Investigating abiotic drivers for vertical and temporal heterogeneities of cyanobacteria concentrations in lakes using a seasonal in situ monitoring station. Water Resour. Res. 55, 954–972.